Tbx2b is required for ultraviolet photoreceptor cell specification during zebrafish retinal development

Karen Alvarez-Delfin[a], Ann C. Morris[a], Corey D. Snelson[b], Joshua T. Gamse[b], Tripti Gupta[c], Florence L. Marlow[c], Mary C. Mullins[c], Harold A. Burgess[c], Michael Granato[c], and James M. Fadool[a,1]

[a]Department of Biological Science and Program in Neuroscience, Florida State University, Tallahassee, FL 32306-4295; [b]Department of Biological Sciences, Vanderbilt University, Nashville, TN 37235-1634; and [c]Department of Cell and Developmental Biology, University of Pennsylvania School of Medicine, Philadelphia, PA 19104-6058

Edited by Constance L. Cepko, Harvard Medical School, Boston, MA, and approved December 11, 2008 (received for review September 21, 2008)

The vertebrate rod and cone photoreceptors are highly specialized sensory neurons that transduce light into the chemical and electrical signals of the nervous system. Although the physiological properties of cones and rods are well known, only a handful of genes have been identified that regulate the specification of photoreceptor subtypes. Taking advantage of the mosaic organization of photoreceptors in zebrafish, we report the isolation of a mutation resulting in a unique change in photoreceptor cell fate. Mutation of the *lots-of-rods* (*lor*) locus results in a near one-for-one transformation of UV-cone precursors into rods. The transformed cells exhibit morphological characteristics and a gene-expression pattern typical of rods, but differentiate in a temporal and spatial pattern consistent with UV-cone development. In mutant larvae and adults, the highly ordered photoreceptor mosaic is maintained and degeneration is not observed, suggesting that *lor* functions after the specification of the other photoreceptor subtypes. In genetic chimeras, *lor* functions cell-autonomously in the specification of photoreceptor cell fate. Linkage analysis and genetic-complementation testing indicate that *lor* is an allele of *tbx2b*/*fby* (*from beyond*). *fby* was identified by a pineal complex phenotype, and carries a nonsense mutation in the T-box domain of the tbx2b transcription factor. Homozygous *fby* mutant larvae and *lor*/*fby* transheterozygotes also display the lots-of-rods phenotype. Based upon these data, we propose a previously undescribed function for *tbx2b* in photoreceptor cell precursors, to promote the UV cone fate by repressing the rod differentiation pathway.

cone | *Danio rerio* | T-box | mosaic

Vertebrates have evolved 2 major classes of retinal photoreceptors: rods, which mediate dim light vision, and cones, which detect light of greater intensity, have a faster temporal resolution, and mediate color vision. Largely from the analysis of mutations in mice and humans, a transcriptional network regulating photoreceptor cell development has been proposed. The presumptive photoreceptor progenitors sequentially express the homeobox transcription factors (TFs) Otx2 and Crx (1–3), and in their absence, photoreceptor precursors are not specified or fail to differentiate. Rod specification requires the additional expression of the Maf-family TF Nrl and its target Nr2e3 (4, 5). Nrl acts as a molecular switch; in its absence, precursors adopt the short-wavelength (S) opsin cone fate (5, 6), and mis- and over-expression of Nrl transforms most if not all cone precursors into functional rods (7, 8). *NR2E3* expression, which is disrupted in enhanced S-cone syndrome in humans and the *rd7* mouse, is required for the repression of cone-specific genes in rod precursors (4, 9, 10). However, it remains to be determined if a reciprocal system exists in cone precursors for repressing rod-specific genes.

The zebrafish retina, in addition to rods, possesses 4 cone subtypes, each with a distinct morphology and expressing a unique opsin (11–17). The spatial and temporal differentiation of the photoreceptors leads to the formation of a highly ordered, precisely defined arrangement (16, 18). The photoreceptor mosaic provides an opportunity to systematically uncover genetic mechanisms regulating vertebrate photoreceptor subtype specification, similar to the studies of *Drosophila* ommatidial assembly initiated several decades ago.

We identified a mutation called *lots-of-rods* ($lor^{p25bbtl}$) that results in an increase in the number of rods and a decrease in the number of UV cones in the larval and adult zebrafish retina. The $lor^{p25bbtl}$ phenotype demonstrates many features opposite to those observed in enhanced S-cone syndrome and mutations of *Nr2e3* or *Nrl* in mice. Genetic analysis revealed that $lor^{p25bbtl}$ is an allele of *tbx2b*, a T-box TF with essential roles in development (19–22). Our data suggest that during photoreceptor cell differentiation, *tbx2b* acts cell-autonomously to promote the UV-cone fate by repressing the rod fate in zebrafish photoreceptor cell progenitors.

Results

To identify genes essential for vertebrate photoreceptor development, we screened 5- to 6-day postfertilization (dpf) zebrafish larvae for ethyl nitrosourea-induced mutations, leading to alterations in rod patterning (23). Rods first appear in the ventral retina coincident with the expression of the first cone opsin (Fig. 1*B*) but differentiate in the dorsal and central retina in a sporadic pattern subsequent to the differentiation of the cones (Fig. 1*C*) (15, 17). In contrast, $lor^{p25bbtl}$ mutants displayed a higher number of rods across the entire retina, with few gaps in the central or dorsal regions (Fig. 1*E*). Between 3 and 5 dpf, rod immunolabeling in mutant larvae spread in a continuous front from the ventral to central and finally to the dorsal retina, reminiscent of the wave-like fashion of cone differentiation (14) (Fig. 1*F*). The increased number of rods was confirmed by labeling with either monoclonal or polyclonal antibodies against rhodopsin, and was mirrored by GFP expression when $lor^{p25bbtl}$ was placed on the *XOPS-GFP* transgenic background (18). In teleosts, rods are continuously added to the postembryonic retina from a population of mitotically active cells called the rod progenitors (24); however, BrdU labeling detected no increased mitotic activity in $lor^{p25bbtl}$ mutants (data not shown). $lor^{p25bbtl}$ mutants were also morphologically normal (Fig. 1 *A* and *D*), demonstrated a robust optokinetic response (OKR), and could be routinely reared to fertile adults.

Author contributions: K.A.-D., T.G., F.L.M., M.C.M., H.A.B., M.G., and J.M.F. designed research; K.A.-D., A.C.M., C.D.S., and J.M.F. performed research; K.A.-D., C.D.S., J.T.G., T.G., F.L.M., M.C.M., H.A.B., M.G., and J.M.F. contributed new reagents/analytic tools; K.A.-D., A.C.M., and J.M.F. analyzed data; and K.A.-D. and J.M.F. wrote the paper.

The authors declare no conflict of interest.

This article is a PNAS Direct Submission.

Freely available online through the PNAS open access option.

[1]To whom correspondence should be addressed. E-mail: jfadool@bio.fsu.edu.

This article contains supporting information online at www.pnas.org/cgi/content/full/0809439106/DCSupplemental.

NEUROSCIENCE

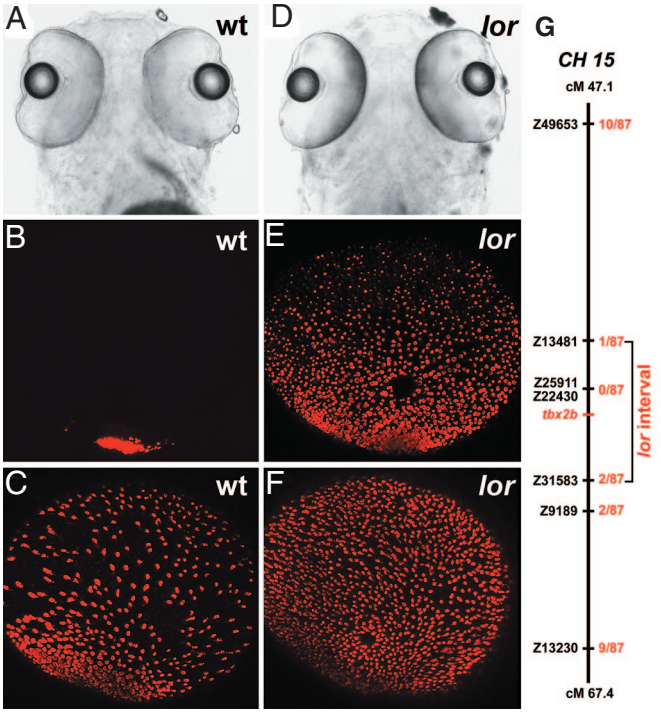

Fig. 1. *lor*^{p25bbtl} mutants display increased labeling for rods. Ventral views of bright field images (*A* and *D*) and confocal immunofluorescent images of rod-specific labeling of eyes from WT (*B* and *C*) and a *lor*^{p25bbtl} mutant larvae (*E* and *F*) (dorsal is up). At 3 dpf, WT larvae display rod labeling first in the ventral retina (*B*) followed at 5 dpf, by sporadic labeling of individual cells in the central and dorsal retina (*C*). At 3 dpf, *lor*^{p25bbtl} mutant larvae display increased rod immunolabeling across the ventral and central retina (*E*) that is evenly distributed at 5 dpf (*F*). (*G*) Linkage analysis placed *lor*^{p25bbtl} between SSLP markers Z31583 and Z13481 on the MGH panel. The number of recombinants in 87 mutant larvae is shown (*red*). The interval containing the *lor* mutation and the *tbx2b* locus is shown.

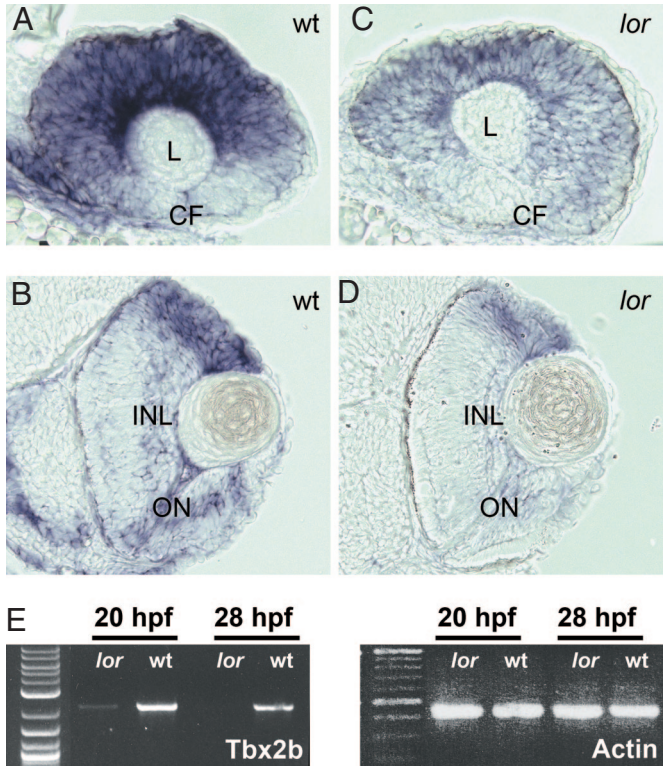

Fig. 2. *tbx2b* expression is reduced in *lor* mutant embryos. Sagittal sections of WT (*A*) and *lor*^{p25bbtl} mutant (*C*) embryos at 28 hours postfertilization (hpf) following in situ hybridization for *tbx2b* show labeling throughout the eye, but the lack of expression in the ventral retina near the choroid fissure (CF) and lens (L). Transverse sections of labeled WT (*B*) and *lor*^{p25bbtl} embryos (*D*) at 44 hpf. *tbx2b* expression is most intense at the dorsal retinal margin and cells adjacent to the developing outer nuclear layer (ONL) as well as the inner nuclear layer (INL) (optic nerve; ON). Note the dramatically reduced expression in the *lor*^{p25bbtl} embryos. (*E*) Amplification of *tbx2b* by RT-PCR from RNA extracted from WT and *lor*^{p25bbtl} embryos at 20 and 28 hpf demonstrates a reduction in the amount of *tbx2b* mRNA in the mutant.

The *lor*^{p25bbtl} mutation was mapped to an interval of chromosome 15, near simple sequence length polymorphism (SSLP) markers z22430/z25911 (Fig. 1*G*), where *tbx4* and *tbx2b*/*fby* were localized (21). *tbx2b* is a TF mainly associated with transcriptional repression during cell cycle control, limb, heart and endoderm development (19, 20, 22), and cancer (25). A single mutant allele of *tbx2b* has been reported in zebrafish. The *fby* mutation results from a T-to-A transversion generating a premature stop codon within the T-box sequence, and was isolated based upon a pineal gland phenotype (21). Complementation testing indicated that *lor*^{p25bbtl} is an allele of *tbx2b*. Crosses between carriers of the *lor*^{p25bbtl} mutation and the *fby* mutation revealed that *fby* failed to complement *lor*^{p25bbtl}; ≈25% of the progeny of the intercross displayed the increased rod phenotype (data not shown). In addition, homozygous *fby* mutant larvae, confirmed by sequencing the *tbx2b* gene, demonstrated the "lots-of-rods" phenotype, whereas phenotypically WT siblings were either homozygous for the WT allele or heterozygous.

tbx2b expression was examined by in situ hybridization in WT and *lor*^{p25bbtl} mutant embryos (Fig. 2 *A–D*). *tbx2b* expression was greater in the dorsal retina and absent in the ventral retina adjacent to the choroid fissure (see Fig. 2 *A* and *B*) (26, 27), the region of precocious rod differentiation in embryos and of highest rod density in larvae (see Fig. 1 *B* and *C*). In *lor*^{p25bbtl} mutants, the dorsal/ventral gradient of *tbx2b* retinal expression was still detectable, but labeling was much fainter than in the WT embryos (see Fig. 2 *B* and *D*). At 44 (Fig. 2*D*) and 60 hpf (data not shown), *tbx2b* expression persisted in the inner retina, in the regions of continued neurogenesis at the retinal margins and cells adjacent to the forming ONL, but was diminished in the central retina. In mutant larvae, labeling was greatly reduced across the retina. RT-PCR of RNA extracted from WT and *lor* mutant embryos confirmed the lower expression of *tbx2b* at 20 and 28 hpf in the mutant (Fig. 2*E*). Sequencing of *tbx2b* cDNA from 4-dpf WT and *lor*^{p25bbtl} larvae revealed no changes in the *tbx2b* coding region (data not shown), suggesting that *lor*^{p25bbtl} represents a mutation in a regulatory sequence.

To test if the increased number of rods resulted from a change in fate of 1 of the 4 cone subtypes, serial sections of larvae from intercrosses of *lor*^{p25bbtl} heterozygotes were co-immunolabeled with 1 of 4 polyclonal antisera to the cone opsins and a rod-specific monoclonal antibody to distinguish mutant from WT larvae [supporting information (SI) Fig. S1]. In the *lor*^{p25bbtl} retinas, labeling for the UV opsin was nearly absent (see Fig. S1*D′*). Immunolabeling for the 3 other cone opsins (see Fig. S1) and markers of other retinal cell types did not reveal any other alteration, nor was increased apoptosis or retinal degeneration found.

Confocal images of eyes enucleated from whole-mount immunolabeled WT and mutant larvae confirmed the significant changes in the number of rods and UV cones (Fig. 3 *A*, *B*, *D*). In WT larvae, the UV cones are regularly spaced across the entire retina with the few rods distributed across the central and dorsal regions (see Fig. 3*A*). In *lor*^{p25bbtl}mutant larvae, rods were

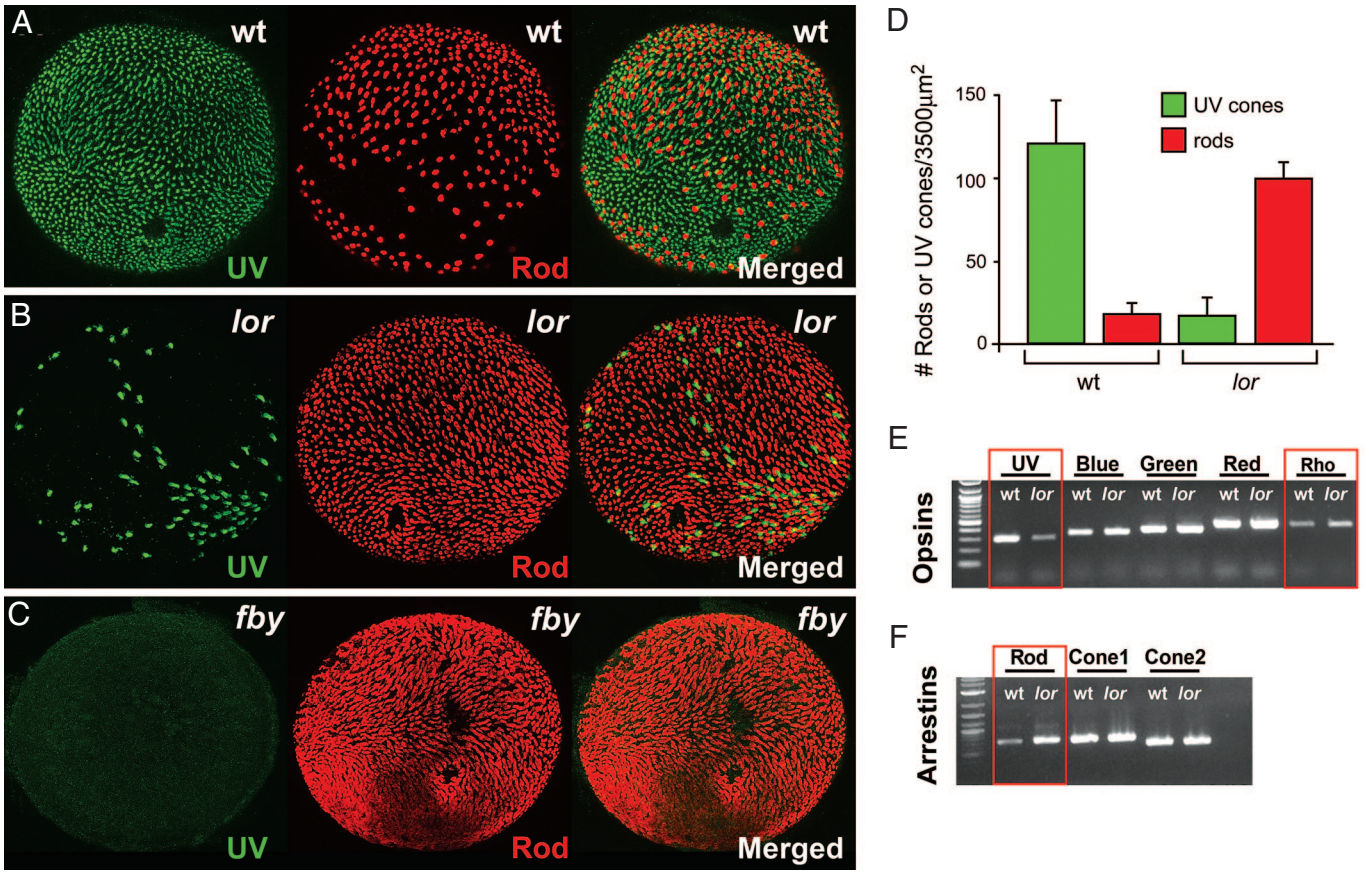

Fig. 3. Increased rod number and fewer UV cones in *lor*^{p25bbtl} and *fby* mutants. (*A–C*) Confocal images of eyes from 5-dpf WT (*A*), *lor*^{p25bbtl} (*B*), and *fby* (*C*) larvae, immunolabeled for UV opsin (*green*) and rods (*red*). Eyes from *lor*^{p25bbtl} and *fby* mutant larvae demonstrate a dramatic deficit in UV cones, with *fby* displaying a more severe phenotype; in this particular sample, no UV cones were detected. (*D*) Graph showing the average number of rods (*red*) and UV cones (*green*) per unit area quantified from confocal images of *lor*^{p25bbtl} mutant and WT retinas (mean + SD). (*E* and *F*) Expression analysis of opsins (*E*) and arrestins (*F*) by RT-PCR from RNA extracted from 5-dpf WT and *lor*^{p25bbtl} larvae. The RT-PCR product for UV opsin was reduced and products for rod opsin and rod arrestin were increased in *lor*^{p25bbtl} (*red boxes*).

evenly distributed across the entire retina and the number of UV cones was markedly reduced (see Fig. 3*B*). The number and distribution of UV cones varied from mutant to mutant and between the 2 eyes from a single animal, and no cells were observed that labeled for both UV opsin and markers of rods simultaneously. Cell counts and spatial pattern analysis of rod labeling in *lor*^{p25bbtl} mutants mirrored those typically observed for the UV cones in WT larvae. Immunolabeling of *fby* mutant larvae revealed a similar yet stronger phenotype (Fig. 3*C*), and transheterozygous larvae (*lor*^{p25bbtl}/*fby*) revealed an intermediate phenotype (Table S1). Expression analysis by RT-PCR of opsins and photoreceptor arrestins in 5-dpf larvae confirmed the increase in expression of rod opsin and rod arrestin and the decrease in expression of the UV opsin in *lor*^{p25bbtl} mutant larvae relative to controls (Fig. 3 *E* and *F*). Based upon the genetic data, we propose that *lor*^{p25bbtl} is a hypomorphic allele of *tbx2b* and together, *fby* and *lor*^{p25bbtl} form an allelic series. Therefore, we shall refer to the *lor*^{p25bbtl} allele as *tbx2b*^{p25bbtl}.

Histological analysis of the photoreceptor cell mosaic was performed in WT and *tbx2b*^{p25bbtl} adults. In transverse sections (Fig. 4 *A* and *C*), other than showing fewer UV cones, *tbx2b*^{p25bbtl} homozygous adults demonstrated no significant difference in laminar organization of the photoreceptors (Fig. 4 *A* and *C*). Rods appeared equally abundant in WT and *lor*, most likely because of the persistent mitotic activity of the rod progenitors. Across the entire retina, the morphology of the rods and remaining UV cones was normal (see Fig. 4*C*). There were no intermediate or hybrid cell types, such as the so-called "cods" or "rones" that occur in the *Nr2e3* mutant mice (4, 28). In tangential sections taken near the outer limiting membrane (OLM), the photoreceptor mosaic was distorted in *tbx2b*^{p25bbtl} adults; the double cone nuclei were not in orderly rows, and the numerous rod inner segments were aggregated together as they passed through the OLM (data not shown). However, more distal sections through the level of the blue-cone inner segments and remaining UV-cone outer segments revealed that the alternating rows of single and double cones were maintained, and the occasional UV cone alternated in rows with the blue cones (Fig. 4*D*). Therefore, the most plausible explanation for the disruption of the mosaic near the OLM is that the physical absence of the UV cones led to a distortion of the orderly packing of the remaining photoreceptors.

Numerous soluble factors have been implicated in the differentiation of rods and cones (29, 30), yet as a TF, we would predict that tbx2b functions cell-autonomously in photoreceptor cell specification. To test this hypothesis, we generated genetic chimeras between WT and *tbx2b*^{p25bbtl} mutant embryos (31). Cells from WT blastula stage embryos (donors) injected with rodamine-dextran were transplanted into age-matched *tbx2b*^{p25bbtl} hosts carrying the *XOPS-GFP* transgene (18). The resulting chimeras displayed retinas with a mixture of donor WT cells among regions of mutant cells with GFP^{+} rods. Immunolabeling for UV opsin and rhodopsin demonstated that the donor-derived WT cells (*red*) often colabeled for UV opsin, but

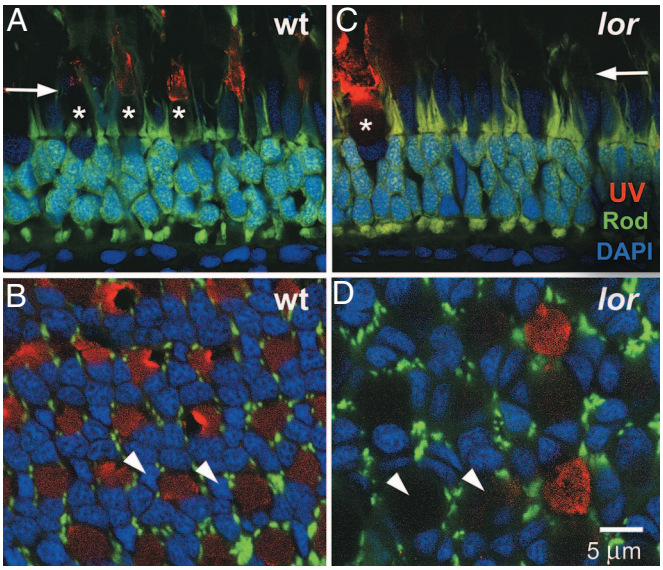

Fig. 4. Maintenance of the photoreceptor mosaic in *tbx2b*^{p25bbtl} mutant adults. Transverse (*A* and *C*) and tangential (*B* and *D*) histological sections through the ONL from WT and *tbx2b*^{p25bbtl} adult animals (rods are GFP^{+}) (*green*), immunolabeled for UV opsin (*red*), and counterstained with DAPI (*blue*). (*A* and *C*) Tiering of the rod and cone photoreceptor cells is maintained although the UV cones (*asterisks*) in the *tbx2b*^{p25bbtl} retinas are diminished in number and appear to have a greater width than in WT retinas. The approximate plane of the sections in (*B*) and (*D*) are indicated [*arrows* in (*A*) and (*C*)]. (*B*) Immunolabeling of tangential sections for the UV opsin reveals the photoreceptor cell mosaic composed of rows of UV cones and blue cones (*arrowheads*). (*D*) In *tbx2b*^{p25bbtl} the regular arrangement of the rows of blue cones (gaps in labeling; *arrowheads*) and occasional UV cones are maintained although the width of the cones is greater and there is some distortion of the row mosaic.

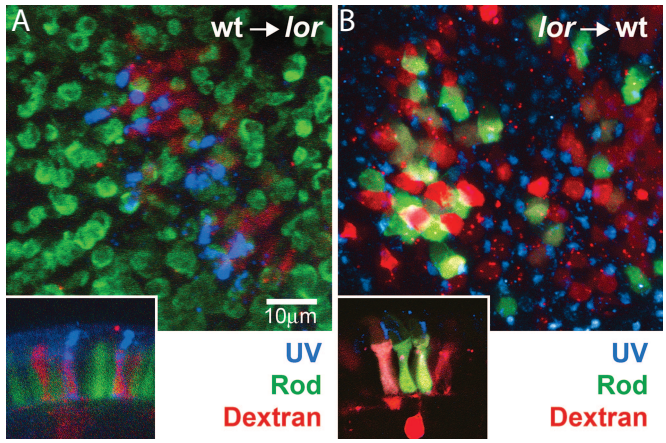

Fig. 5. *tbx2b*^{p25bbtl} acts cell-autonomously. Genetic chimeras were generated by blastula transplantation and allowed to develop to 80 hpf. Donor cells were labeled by rhodamine-dextran (*red*); *tbx2b*^{p25bbtl} deficient rods expressed the XOPS-GFP transgene. Chimeras were whole-mount immunolabeled for UV opsin (*A* and *B*) (*blue*) and for rods (*A*) (*green*). (*A* and *B*) Stacks of confocal images taken tangential to the photoreceptor cell layer and in the orthogonal plane (*insets*). (*A*) WT donor cells (*red*) located in the ONL of *tbx2b*^{p25bbtl} hosts frequently colabel for the UV opsin (*inset*). (*B*) *tbx2b*^{p25bbtl} mutant donor cells (*red*) in the ONL of WT hosts frequently differentiate as GFP^{+} rods and rarely label for the UV opsin. Inset shows dextran/GFP positive rods neighboring UV opsin-positive/dextran negative cone outer segments.

few colabeled for rod opsin (Fig. 5*A*). In contrast, among the neighboring mutant cells, UV-opsin expression was absent and GFP^{+} rods were abundant (see Fig. 5*A*). In 4 mutant retinas, cell counts showed of the 113 WT donor cells located in the ONL, 44 cells (39%) colabeled for UV opsin, and only 9 (8%) for rod opsin. In reciprocal transplants, out of 148 *tbx2b*^{p25bbtl} mutant donor cells, 5 cells (3.4%) colabeled for UV opsin and 65 cells (44%) colabeled for rod opsin (Fig. 5*B*), consistent with a cell-autonomous role in regulating photoreceptor cell fate.

Nr2e3, an early marker and key regulator of rod differentiation in most vertebrates, is transiently expressed in all presumptive photoreceptors in the zebrafish; then, before the onset of opsin expression, Nr2e3 becomes restricted to cells of the rod lineage (4, 32). As such, we would anticipate that in *tbx2b*^{p25bbtl} mutant larvae, Nr2e3 expression would persist in the population of progenitors transfated to become rods. Immunofluorescent images of WT retinas showed that at 2 dpf, before genesis of the ONL, cells in the central retina and near the future ONL expressed Nr2e3 (Fig. 6*A*). By 3 dpf, almost all of the Nr2e3 labeling was restricted to the ONL, and as the first rods started developing in the ventral retina, colocalization of nuclear labeling for Nr2e3 and rod labeling was detected (Fig. 6*B Inset*). As previously reported (4), by 4 dpf the expression of Nr2e3 was down-regulated in the presumptive cones and became restricted to cells sporadically distributed across the ONL that colabeled for rod opsin (Fig. 6*C*). Near the retinal margin, individual cells expressing Nr2e3 and not colabeled for the rod marker can be observed. In *tbx2b*^{p25bbtl} mutants, Nr2e3 expression persisted in many cells across the ONL, most of which colabeled for rod markers (Fig. 6*D*). These data suggest that the reduction or absence of *tbx2b* leads to the persistent expression of Nr2e3 in a subset of cells and their subsequent differentiation as rods.

Discussion

Taking advantage of the precisely defined photoreceptor mosaic in zebrafish, the data show that *lor*^{p25bbtl} mutants exhibit an increase in the number of rods and a dramatic decrease in the number of UV cones because of a change in cell fate. We present genetic evidence that *tbx2b* is a regulator of photoreceptor cell fate in zebrafish and is essential for the proper specification of the UV cone. Most striking is that the function of *tbx2b* during photoreceptor development is opposite to that of Nrl (5).

Our data significantly add to the most widely held model of neuronal specification during retinal development. The current model proposes that multipotent retinal progenitor cells pass through a series of competence states, such that at a specific time, cells can adopt only one or a few particular cell fates in response to extrinsic signals or internal cues (33). Consistent with this model, early- and late-born photoreceptor cell progenitors express the TFs Otx, Crx, and NeuroD (1–3, 34). Yet, in early-born photoreceptor cell precursors, thyroid hormone receptor beta regulates the expression of middle wavelength-sensitive opsin versus S-opsin (29), and in later-born precursors, Nrl acts as a molecular switch to drive expression of rod genes and repress the S-cone fate (5, 6). Thus, the S-cone was positioned as the default photoreceptor. Our data identify a previously unknown pathway essential for specification of the UV cone fate, the likely homologue of the S-cone in mammals. Previous studies have described Tbx2 as a transcriptional repressor (19, 20, 25). Based upon these observations, we propose a mechanism by which photoreceptor cell diversity is maintained by the expression of discrete genes that act to suppress alternative cell fates within precursors that share a common molecular signature.

What can be concluded about this strikingly conserved relationship between SWS1-cone precursors and rod progenitors in teleosts and mammals? As noted, the phenotype observed by mutation of *tbx2b* in zebrafish is directly opposite to the phenotype elicited by loss of *Nrl* function in mammals, suggesting a

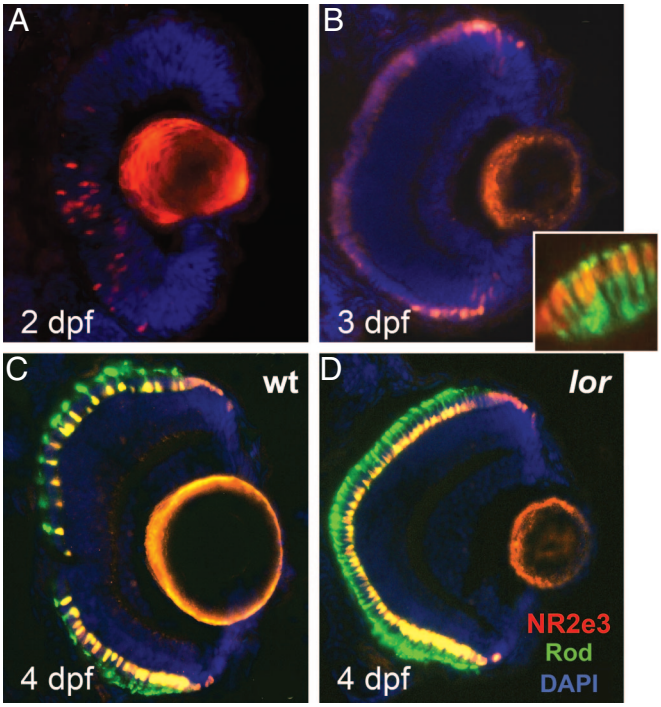

Fig. 6. Persistent Nr2e3 expression in *lor*. (*A–D*) Transverse cryosections from 2- (*A*), 3- (*B*), and 4-dpf (*C* and *D*) WT and *tbx2b*^{p25bbtl} embryos immunolabeled for rods (4C12, *green*) and Nr2e3 (*red*), and counterstained with DAPI (*blue*); dorsal is up. (*A*) At 2 dpf, labeling for Nr2e3 is observed in the inner and outer retina before differentiation of photoreceptors. (*B*) At 3 dpf, Nr2e3 labeling is restricted to developing photoreceptors in the ONL. In the ventral retina, Nr2e3 nuclear labeling colocalizes with immunolabeling for rods (*inset*). (*C* and *D*) At 4 dpf, expression of Nr2e3 persists in differentiating rods in WT and *tbx2b*^{p25bbtl} retinas.

conserved ontology. The evidence suggests that *tbx2* orthologues may also play a role in photoreceptor identity in mammals. Consistent with the genetic data, the dorsal-ventral pattern of expression of *Tbx2* in the retina is remarkably conserved across vertebrates, suggesting a conservation of function (26, 27, 35–37). Additionally, a search for genetic modifiers of the *rd7* mouse uncovered several loci that suppress the retinal degeneration and restore the normal photoreceptor number (38). One of these mapped to chromosome 11, in close proximity to the *Tbx2* locus. Moreover, as part of an *in silico* study of human promoter sequences, *TBX2* was identified as a potential target for the photoreceptor-specific TFs NRL, NR2E3, and CRX (39). Unfortunately, targeted mutagenesis of *Tbx2* in mice causes severe cardiac defects (20), and mutant embryos die between embryonic day 10.5 and 14.5, preventing an analysis of photoreceptor cell fate.

The dorsal-ventral gradient of tbx2b expression and its conspicuous absence from the ventral retina, an area of precocious rod genesis in zebrafish, suggests that the function of tbx2b is to repress the rod cell fate. Consistent with this hypothesis, the reduction or absence of tbx2b expression in genetic mutants underlies the precocious differentiation of rods across the entire retina. The expression data suggest that the timing of *tbx2b* action precedes photoreceptor differentiation. *tbx2b* mRNA is expressed in the neuroepithelium and at the retinal margin before formation of the ONL, yet is down-regulated in photoreceptors. Similarly, we report that Nr2e3 expression is observed in cells of the central retina before formation of the ONL, at the retinal margin, and is expressed by mitotic photoreceptor progenitors (32). In addition, others have shown that *Crx* and *NeuroD* are also expressed in a comparable pattern (34, 40). Thus, in a rapidly developing vertebrate such as the zebrafish, photoreceptor specification may occur before or be coincident with cell cycle exit and laminar positioning. Interestingly, prior work suggested that *tbx2b* is essential for neuronal differentiation in the dorsal retina (26), but we did not find evidence for a similar defect in homozygous *tbx2b*^{p25bbtl} or *fby* mutant larvae. However, a second zebrafish orthologue of mammalian tbx2, tbx2a (also called tbx2b-like), shares 78% identity with *tbx2b* (41) and shows a similar pattern of expression. The previously reported morpholino experiments likely revealed a conserved role for tbx2 orthologues during the earlier stages of vertebrate retinogenesis.

In summary, our unique finding for *tbx2b* in zebrafish is one of only a small collection of studies in vertebrates, to show a specific role for a TF in photoreceptor-cell subtype specification. The phenotype also suggests a highly conserved relationship between rod progenitors and the SWS1-cone precursors in teleost and mammals. It is anticipated that as genetic screens for alterations in the teleost retinal mosaic continue, additional genes that regulate vertebrate photoreceptor subtype specification will be isolated and allow us to test specific hypotheses of the mechanisms of cell fate determination in the nervous system.

Methods

Zebrafish Maintenance. Rearing, breeding, and staging of zebrafish (*Danio rerio*) were performed according to standard methods (42). The *tbx2b*^{p25bbtl} mutant was isolated from a screen of ethyl nitrosourea-mutagenized zebrafish immunolabeled for developing rods at 5 to 6 dpf (23). Mutagenesis was performed at the University of Pennsylvania as previously described (43). The transgenic zebrafish line expressing GFP in rods (18) and the *fby*^{c144} line were previously described (21). All procedures were approved by the Florida State University Animal Care and Use Committee.

PCR, Cloning, and Sequencing. Primers for cloning the ORF of *tbx2b* were provided by Dr. Jeffrey Gross. RNA was isolated with TRIzol (Life Technologies), and cDNA was synthesized using oligo(dT) primer. The sequences of the gene specific primers can be provided upon request. The RT-PCR products from 4-dpf WT and *tbx2b*^{p25bbtl} embryos were cloned into the TOPO vector (Invitrogen) and sequenced.

The amplification and sequencing of the T-box in the *tbx2b* gene from the *fby* line was performed as follows: The progeny of *fby* heterozygous parents were fixed at 5 dpf, immunolabeled with 4C12 antibody (specific for rods), and screened for WT and ''lots-of-rods'' phenotype. DNA was extracted from 3 individual larva of each condition and subjected to PCR. The 1,603-bp PCR product was sequenced and the resulting data for WT and *tbx2b*^{p25bbtl} were compared.

Immunohistochemistry. Immunolabeling and fluorescence microscopy of whole-mount larvae and frozen sections (10 μm) were performed as described previously (18, 44). BrdU incorporation was performed as described (32). Sections and enucleated eyes from whole-mounted immunolabeled larvae were imaged with a Zeiss 510 Scanning Laser Confocal microscope equipped with either a 20× (NA 0.75) objective or 40× water-immersion objective (NA 1.2) as described (18).

Whole-Mount in Situ Hybridization. Whole-mount in situ hybridization was performed essentially as described (45).

Cell Transplantation. Genetic chimeras were generated as described (31). Donors were labeled at the 1- and 2-cell stage by injection with lysine-fixable dextran-conjugated Alexa Fluor 594 (Invitrogen). Transplant was performed at the 1,000-cell stage. The chimeras were fixed at 80 hpf and immunolabeled as described above.

Mapping. Linkage analysis was performed at the Zebrafish Mapping Facility at the University of Louisville from DNA isolated from 100 WT siblings and 100 *tbx2b*^{p25bbtl} embryos using SSLP markers (46).

Quantitative Analysis. Confocal images from whole eyes immunolabeled for UV cones and rods (4C12 antibody) were analyzed with the Scion Image Software (Scion) (18). An area corresponding to 3,500 μm^2 in the central retina was used to count UV cones and rods in 4- and 5-dpf WT and *lor* retinas. The

following number (*n*) of 4- or 5-dpf retinas and cells types were analyzed: WT, $n = 4$ (UV cones) and $n = 6$ (rods); *tbx2b*^{p25bbtl}, $n = 6$ (UV cones) and $n = 6$ (rods); *lor/fby*, $n = 7$ (UV cones and rods). The average number of UV cones or rods and the standard deviation were reported.

ACKNOWLEDGMENTS. We thank Tamera Scholz, Gina Rockholt, and Katie Lewis for fish care, Charles Badland for assistance with preparation of the figures, Anne Thistle for editorial assistance, and the staff of the Florida State University Biological Imaging facility. We thank Jeremy Nathans and David Hyde for reagents and Ronald Gregg for initial mapping of *lor*^{p25bbtl}. This work was supported by a Planning Grant from Florida State University (to J.M.F.), and National Institutes of Health Grants R01EY017753 (to J.M.F.), R01HD054534 (to J.T.G.), R01MH075691 (to M.G.), and R01HD050901 (to M.C.M). The Zebrafish Mapping Facility at the University of Louisville is supported by Grant R01RR020357 (to Ronald Gregg).

1. Freund CL, *et al.* (1997) Cone-rod dystrophy due to mutations in a novel photoreceptor-specific homeobox gene (CRX) essential for maintenance of the photoreceptor. *Cell* 91:543–553.
2. Furukawa T, Morrow EM, Cepko CL (1997) *Crx*, a novel otx-like homeobox gene, shows photoreceptor-specific expression and regulates photoreceptor differentiation. *Cell* 91:531–541.
3. Nishida A, *et al.* (2003) *Otx2* homeobox gene controls retinal photoreceptor cell fate and pineal gland development. *Nat Neurosci* 6:1255–1263.
4. Chen J, Rattner A, Nathans J (2005) The rod photoreceptor-specific nuclear receptor Nr2e3 represses transcription of multiple cone-specific genes. *J Neurosci* 25:118–129.
5. Mears AJ, *et al.* (2001) Nrl is required for rod photoreceptor development. *Nat Genet* 29:447–452.
6. Akimoto M, *et al.* (2006) Targeting of GFP to newborn rods by nrl promoter and temporal expression profiling of flow-sorted photoreceptors. *Proc Natl Acad Sci USA* 103:3890–3895.
7. McIlvain VA, Knox BE (2007) Nr2e3 and nrl can reprogram retinal precursors to the rod fate in xenopus retina. *Dev Dyn* 236:1970–1979.
8. Oh EC, *et al.* (2007) Transformation of cone precursors to functional rod photoreceptors by bZIP transcription factor NRL. *Proc Natl Acad Sci USA* 104:1679–1684.
9. Akhmedov NB, *et al.* (2000) A deletion in a photoreceptor-specific nuclear receptor mRNA causes retinal degeneration in the *rd7* mouse. *Proc Natl Acad Sci USA* 97:5551–5556.
10. Haider NB, *et al.* (2000) Mutation of a nuclear receptor gene, *NR2E3*, causes enhanced S cone syndrome, a disorder of retinal cell fate. *Nat Genet* 24:127–131.
11. Branchek T, Bremiller R (1984) The development of photoreceptors in the zebrafish, *brachydanio rerio*. I. Structure. *J Comp Neurol* 224:107–115.
12. Branchek T (1984) The development of photoreceptors in the zebrafish, *brachydanio rerio*. II. Function. *J Comp Neurol* 224:116–122.
13. Larison KD, Bremiller R (1990) Early onset of phenotype and cell patterning in the embryonic zebrafish retina. *Development* 109:567–576.
14. Raymond PA, Barthel LK, Rounsifer ME, Sullivan SA, Knight JK (1993) Expression of rod and cone visual pigments in goldfish and zebrafish: A rhodopsin-like gene is expressed in cones. *Neuron* 10:1161–1174.
15. Raymond PA, Barthel LK, Curran GA (1995) Developmental patterning of rod and cone photoreceptors in embryonic zebrafish. *J Comp Neurol* 359:537–550.
16. Robinson J, Schmitt EA, Harosi FI, Reece RJ, Dowling JE (1993) Zebrafish ultraviolet visual pigment: Absorption spectrum, sequence, and localization. *Proc Natl Acad Sci USA* 90:6009–6012.
17. Schmitt EA, Dowling JE (1996) Comparison of topographical patterns of ganglion and photoreceptor cell differentiation in the retina of the zebrafish, *danio rerio*. *J Comp Neurol* 371:222–234.
18. Fadool JM (2003) Development of a rod photoreceptor mosaic revealed in transgenic zebrafish. *Dev Biol* 258:277–290.
19. Christoffels VM, *et al.* (2004) T-box transcription factor Tbx2 represses differentiation and formation of the cardiac chambers. *Dev Dyn* 229:763–770.
20. Harrelson Z, *et al.* (2004) Tbx2 is essential for patterning the atrioventricular canal and for morphogenesis of the outflow tract during heart development. *Development* 131:5041–5052.
21. Snelson CD, Santhakumar K, Halpern ME, Gamse JT (2008) Tbx2b is required for the development of the parapineal organ. *Development* 135:1693–1702.
22. Fong SH, Emelyanov A, Teh C, Korzh V (2005) Wnt signalling mediated by Tbx2b regulates cell migration during formation of the neural plate. *Development* 132:3587–3596.
23. Morris AC, Fadool JM (2005) Studying rod photoreceptor development in zebrafish. *Physiol Behav* 86:306–313.
24. Johns PR, Fernald RD (1981) Genesis of rods in teleost fish retina. *Nature* 293:141–142.
25. Jacobs JJ, *et al.* (2000) Senescence bypass screen identifies TBX2, which represses Cdkn2a (p19(ARF)) and is amplified in a subset of human breast cancers. *Nat Genet* 26:291–299.
26. Gross JM, Dowling JE (2005) Tbx2b is essential for neuronal differentiation along the dorsal/ventral axis of the zebrafish retina. *Proc Natl Acad Sci USA* 102:4371–4376.
27. Ruvinsky I, Oates AC, Silver LM, Ho RK (2000) The evolution of paired appendages in vertebrates: T-box genes in the zebrafish. *Dev Genes Evol* 210:82–91.
28. Corbo JC, Cepko CL (2005) A hybrid photoreceptor expressing both rod and cone genes in a mouse model of enhanced S-cone syndrome. *PLoS Genet* 1:e11.
29. Ng L, *et al.* (2001) A thyroid hormone receptor that is required for the development of green cone photoreceptors. *Nat Genet* 27:94–98.
30. Levine EM, Fuhrmann S, Reh TA (2000) Soluble factors and the development of rod photoreceptors. *Cell Mol Life Sci* 57:224–234.
31. Link BA, Fadool JM, Malicki J, Dowling JE (2000) The zebrafish young mutation acts non-cell-autonomously to uncouple differentiation from specification for all retinal cells. *Development* 127:2177–2188.
32. Morris AC, Scholz TL, Brockerhoff SE, Fadool JM (2008) Genetic dissection reveals two separate pathways for rod and cone regeneration in the teleost retina. *Dev Neurobiol* 68:605–619.
33. Cepko CL, Austin CP, Yang X, Alexiades M, Ezzeddine D (1996) Cell fate determination in the vertebrate retina. *Proc Natl Acad Sci USA* 93:589–595.
34. Morrow EM, Furukawa T, Lee JE, Cepko CL (1999) NeuroD regulates multiple functions in the developing neural retina in rodent. *Development* 126:23–36.
35. Gibson-Brown JJ, I Agulnik S, Silver LM, Papaioannou VE (1998) Expression of T-box genes *Tbx2-Tbx5* during chick organogenesis. *Mech Dev* 74:165–169.
36. Hayata T, Kuroda H, Eisaki A, Asashima M (1999) Expression of xenopus T-box transcription factor, tbx2 in xenopus embryo. *Dev Genes Evol* 209:625–628.
37. Sowden JC, Holt JK, Meins M, Smith HK, Bhattacharya SS (2001) Expression of *drosophila omb*-related T-box genes in the developing human and mouse neural retina. *Invest Ophthalmol Vis Sci* 42:3095–3102.
38. Haider NB, *et al.* (2008) Mapping of genetic modifiers of Nr2e3 rd7/rd7 that suppress retinal degeneration and restore blue cone cells to normal quantity. *Mamm Genome* 19:145–154.
39. Qian J, *et al.* (2005) Identification of regulatory targets of tissue-specific transcription factors: Application to retina-specific gene regulation. *Nucleic Acids Res* 33:3479–3491.
40. Nelson SM, Frey RA, Wardwell SL, Stenkamp DL (2008) The developmental sequence of gene expression within the rod photoreceptor lineage in embryonic zebrafish. *Dev Dyn* 237:2903–2917.
41. Ribeiro I, *et al.* (2007) Tbx2 and Tbx3 regulate the dynamics of cell proliferation during heart remodeling. *PLoS ONE* 2:e398.
42. Westerfield M (1995) *The Zebrafish Book* (University of Oregon Press, Eugene).
43. Dosch R, *et al.* (2004) Maternal control of vertebrate development before the mid-blastula transition: Mutants from the zebrafish I. *Dev Cell* 6:771–780.
44. Morris AC, Schroeter EH, Bilotta J, Wong RO, Fadool JM (2005) Cone survival despite rod degeneration in XOPS-mCFP transgenic zebrafish. *Invest Ophthalmol Vis Sci* 46:4762–4771.
45. DeCarvalho AC, Cappendijk SL, Fadool JM (2004) Developmental expression of the POU domain transcription factor brn-3b (Pou4f2) in the lateral line and visual system of zebrafish. *Dev Dyn* 229:869–876.
46. Gregg RG, Willer GB, Fadool JM, Dowling JE, Link BA (2003) Positional cloning of the young mutation identifies an essential role for the brahma chromatin remodeling complex in mediating retinal cell differentiation. *Proc Natl Acad Sci USA* 100:6535–6540.